Hindawi
Geofluids
Volume 2024, Article ID 1113144, 14 pages
https://doi.org/10.1155/2024/1113144

Research Article

Creep Energy Evolution of Red-Bed Soft Rocks in South China under Chemical-Stress-Seepage Coupling

Shuguang Zhang,[1] **Fanyao Peng**,[1] **Yingbo Li**,[2] **Zhifeng Liu**,[3] **and Wenbo Liu**[4]

[1]*College of Civil Engineering, Guilin University of Technology, Guilin, Guangxi 541004, China*
[2]*Shenzhen Railway Investment and Construction Group Co., LTD, Shenzhen, Guangdong 518000, China*
[3]*China Railway 16th Bureau Group Co., LTD, Beijing 100018, China*
[4]*Guangxi Key Laboratory of Rock and Soil Mechanics and Engineering, Guilin, Guangxi 541004, China*

Correspondence should be addressed to Shuguang Zhang; zhangsg@glut.edu.cn

Received 27 November 2023; Revised 19 March 2024; Accepted 17 April 2024; Published 29 April 2024

Academic Editor: Paola Cianfarra

The red-bed soft rocks in South China have obvious creep characteristics and are prone to engineering geological disasters such as landslide and foundation settlement under the action of rainfall, groundwater, and load. In order to reveal its creep characteristics and mechanism under complex conditions, a step-loading creep test was carried out under chemical-stress-seepage coupling, and the energy evolution law of the whole creep process was analyzed based on linear energy storage and energy dissipation theory. The results also show that the acid chemical solution has the greatest influence on the triaxial strength and creep strength, and the creep damage and energy evolution of red-bed soft rock are universal. The creep damage and total strain increase with the increase of acidity, the decrease of confining pressure, and the increase of seepage pressure. The evolution law of creep damage shows the characteristics of slow-acceleration-rapid growth, and with the increase of load level, it has obvious transfer and accumulation. After entering the constant velocity creep stage, the damage rate begins to accelerate. The proportion of instantaneous strain and creep strain in the total strain increment is about 50%, and confining pressure has little influence on their respective proportions. The instantaneous strain is more sensitive to the acidity of the chemical solution, and the proportion of creep strain increases gradually with the increase of seepage pressure. The relationship between elastic energy density and total energy density is linear. The elastic energy density and dissipated energy density in the loading stage and creep stage all increase nonlinearly with loading time. The density of dissipated energy in the creep phase is lower than that in the loading phase, but the opposite is true in the higher stress phase, and the law of energy dissipation can explain the hardening damage effect in the creep process of soft rock samples. The research results provide a new perspective for us to reveal the mechanical properties and failure mechanism of red-bed soft rocks and provide an important theoretical basis for predicting and evaluating the creep instability and long-term stability of such rocks.

1. Introductory

Red-bed soft rock, as a common geotechnical engineering soil type in south China, has high porosity, strong hydrophilic character, and obvious creep characteristics [1]. These features bring some challenges to its engineering applications. As a constantly changing complex chemical solution, groundwater plays a key role in the engineering geological environment. Under the seepage and erosion of groundwater, the mechanical properties of the red-bed soft rock will gradually weaken, which may lead to engineering geological disasters such as rock mass landslide, foundation settlement, and slip damage [2, 3]. Once these disasters occur, they will pose a serious threat to people's lives, safety, and property, so it is very important to study the stability of the red-bed soft rock.

Under the action of multiple physical field coupling, the stability of the red-bed soft rock slope is affected by the more complex. The coupling of multiple physical fields makes the mechanical properties of the red-bed soft rock further

change, which puts forward higher requirements to ensure the stability and safety of the project [4]. Therefore, it is an important task to study the stability of the red-bed soft rock slope under multiple physical field coupling.

The influence of hydrorock interaction and chemical corrosion on the physical and mechanical properties of red-bed soft rocks cannot be ignored. The influence of hydrorock interaction on red-bed soft rock is mainly manifested as the pore change from flat to slender, reduced shape factor, and more complex pore structure of [5]. Moreover, the NMR test results of the chemical solution corrosion action samples showed that the internal pore structure change is the root cause of the damage [6]. Through the quantitative analysis of micro, medium, and macroscale of red-bed soft rock destruction, the main role of red-bed soft rock is chemical action. The chemical corrosion damage situation is positively correlated with the concentration of the chemical medium and the acidic strength of the solution [7]. Scholars have further revealed the correlation of the microscopic structure and the macroscopic mechanical parameters by considering the chemical corrosion effect [8, 9]. Therefore, the chemical solution has an obvious weakening effect on the rock's strength.

The red-bed soft rock, as a member of the soft rock family, also shows the obvious creep feature under the long-term water-rock interaction [10]. This creep characteristic is particularly evident in the condition of the flow-solid coupling state. Specifically, the response of radial creep deformation to axial creep deformation will lag behind when the stress level and the seepage pressure remain relatively low. However, under the dual action of high-stress level and osmotic pressure, the creep rate is significantly accelerated, and the duration is also constantly shortened by [11]. In addition, under the action of corrosion damage, the internal structure and mechanical characteristics of the red-bed soft rock have been subjected to different degrees of damage deterioration, making the creep mechanical behavior of the red-bed soft rock become more complex. The time effect of creep and the effect of stress disturbance make the creep mechanical behavior of red-bed soft rocks more difficult to predict and understand [12]. In order to better reveal the complex phenomenon of rock creep destruction, the energy theory to analyze the law of rock damage is gradually recognized by the majority of scholars [13].

The application of energy theory in rock mechanics was originally used to analyze structural damage. Based on a lot of studies on energy conversion, the energy criterion for judging the damage to rock structure was proposed [14, 15]. Subsequently, the study of energy evolution characteristics and energy dissipation in the process of rock loading was gradually deepened, the damage variable and energy storage coefficient based on the energy dissipation theory were proposed, and the quantitative characterization of internal energy storage and dissipation was realized [16, 17]. In recent years, through extensive analysis of the energy dissipation law of the rock addition and unloading test process, it is found that there is a linear relationship between the elastic energy and dissipation energy density of the loading process and the total input energy density, namely, the linear energy storage law [18–20], while an increase in the number of cycles during the loading and unloading tests will reduce the rock energy storage limit [21]. Through comparative analysis of the uniaxial cycle and unloading test, grading loading creep test and creep and unloading test results found that the creep process has no effect on elastic energy density, puts forward the energy evolution of rock creep damage, which provides a new idea for the calculation of creep process energy density, and put forward a method can effectively predict the damage stress [22–24].

The above study shows that the establishment of a red-bed soft rock damage criterion based on energy evolution can reveal the creep damage and damage mechanism of red-bed soft rock [25]. Due to the complexity of the engineering geological environment in South China, the creep process of the chemical environment, stress state, and the comprehensive effect of groundwater seepage under the conditions of creep characteristics, damage evolution, and energy dissipation characteristics remains to be a lot of research [26–28] and reveals that the internal mechanism of soft rock engineering geological disaster prevention is of great significance.

Most of the studies on creep energy evolution currently use the test method of loading and unloading to analyze the rock, and there is a lack of research on the energy evolution law of the triaxial graded loading creep test. In this paper, based on the engineering geological environment of South China, different chemical, stress, and seepage experimental conditions are designed to carry out the graded loading creep test of red-bed soft rock. By analyzing the energy transformation in the creep process of red-bed soft rock, we find that it has a unique law of energy evolution. In each creep stage, the elastic energy and dissipative energy of a rock show different characteristics and influence each other. This law of energy damage evolution provides a new perspective for us to reveal the mechanical properties and failure mechanism of rocks. At the same time, our results also show that the creep deformation and energy dissipation characteristics of red-bed soft rocks under complex environmental conditions are universal, which provides an important theoretical basis for predicting and evaluating the creep instability and long-term stability of such rocks.

2. Triaxial Compression Test

The experimental red-bed soft rock is collected from a construction site in Quanzhou, Guilin, as shown in Figure 1, and the XRD composition test indicates that it is made of quartz, plagiospar, potassium feldspar, and a small amount of dolomite. The main chemical components are silica, iron oxide, calcium oxide, alumina, etc., which belong to the weathered sandy rock class. However, the test samples are processed into standard cylindrical specimens with 100 mm height and 50 mm diameter according to the rock mechanics test specification, and the surface is polished and smooth to make standard test samples, as shown in Figure 2. The dry density of the specimens was tested to be 2.18-2.27 g/cm^3, and the porosity was 6.58-7.01%.

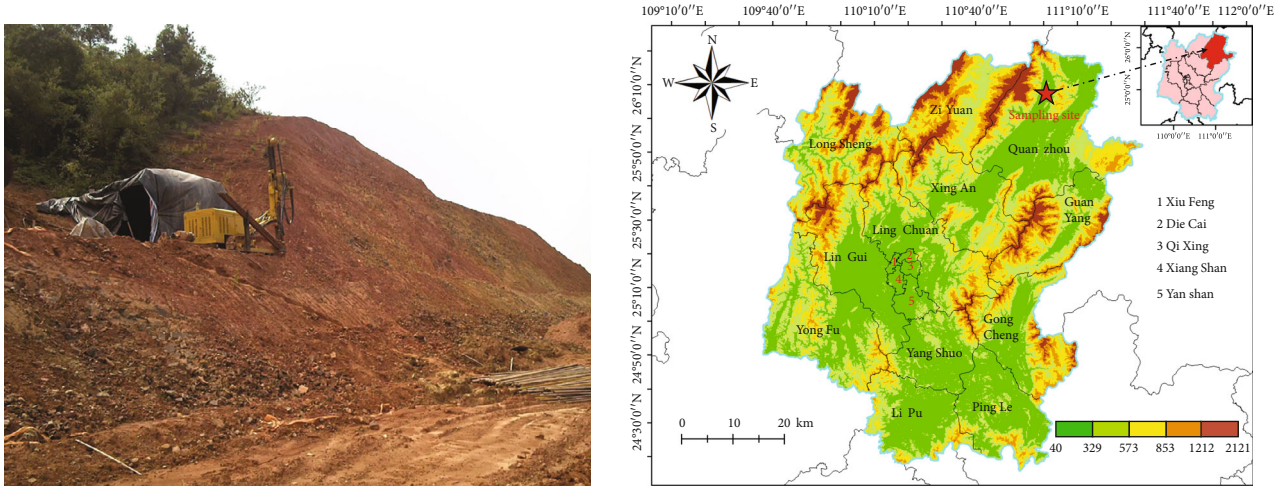

Figure 1: Overview of sampling site locations.

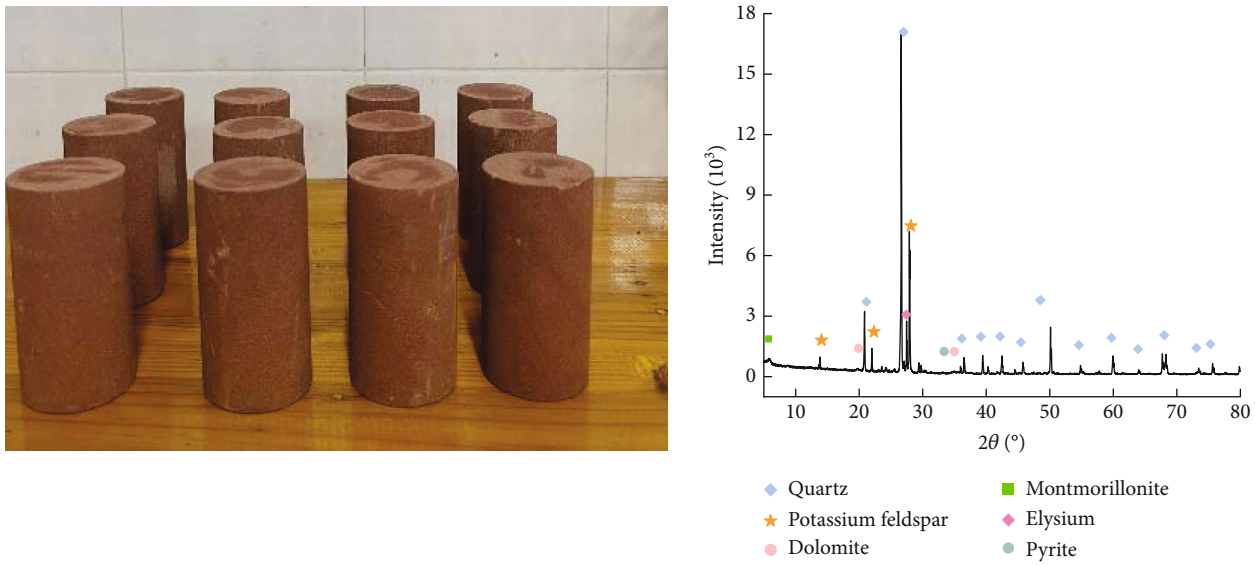

Figure 2: Red-bed soft rock specimens and their XRD diffraction patterns.

The equipment used in the test is a rock-automatic triaxial instrument, as shown in Figure 3. The equipment is jointly developed by the Wuhan Institute of Rock and Soil Mechanics, Chinese Academy of Sciences, and Guilin University of Technology by axial pressure, confining pressure, temperature, air permeability, liquid permeability, and dynamic load, composed of six sets of independent control modules. The maximum axial force of 2000 kN, the maximum confining pressure of 60 MPa, and the maximum seepage pressure of 60 MPa can be provided. It has a variety of load or displacement control modes and can be an arbitrary conversion function, a rock solid-liquid-gas-heat multifield coupling mechanic test.

2.1. Test Program and Steps. In order to determine the stress value of each stage of the creep test under different experimental conditions, the triaxial compression mechanical characteristics of the sample were first tested. The test was divided into three groups: A, B, and C. The sulfuric acid solution with different pH values was used to simulate the chemical environment of the sample. The stress and seepage were realized by applying different confining pressures and seepage pressures, respectively. In group A, the conditions are the same confining pressure and seepage pressure and the different pH values of sulfuric acid solution. In group B, the seepage pressure and solution pH are the same with different confining pressures. In group C, the same confining pressure, solution pH, and seepage pressure are different. In the triaxial compression test, the confining pressure is applied to the preset value at a loading rate of 0.05 MPa/s, and then the axial load is applied to the specimen failure at a loading rate of 0.5 MPa/s. Three rock samples were selected for testing under each test condition. The measured stress-strain curves are shown in Figure 4, and the average strength is shown in Table 1.

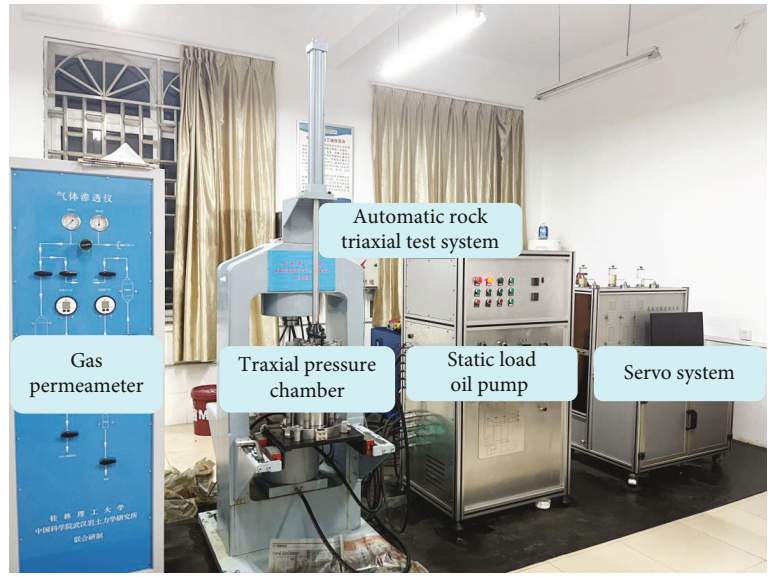

Figure 3: Automatic rock triaxial test system.

In the same stress state, with the decrease of pH value, the reaction between the solution and the internal mineral of the sample intensifies, resulting in the destruction of the internal structure and pore increase, the decrease of peak strength and elastic modulus, and the increase of plastic deformation ability and peak strain. With the increase of the same pH solution, the radial deformation of the red-bed soft rock is inhibited, and the elastic modulus, peak strength, and peak strain all increase, but the difference in the changing trend of the experimental curve is the least, indicating that the elastic modulus does not change much. Under the condition of certain confining pressure, the seepage pressure increases, which continuously reduces the effective stress of the fine particle structure, and the particle fluidity increases, resulting in the reduction of the peak strength of red-bed soft rock. These characteristics are consistent with the results of other scholars and will not be repeated.

3. Creep Characteristic Test

The creep test uses the stage loading method. According to the experimental results of triaxial loading under different test conditions, the applied load of the creep test is divided into 5 stages, which are 40%, 50%, 60%, 70%, and 80% of the maximum deviational stress in order. The specific experimental scheme is as follows: first, apply a small axial pressure, then load the confining pressure to the set value at a rate of 0.1 MPa/s, then open the seepage control valve to pass pure water into the water inlet at the upper end of the three-axis gripper, so that the water inlet pressure is maintained at the preset value of the experiment, and keep for a certain time until the specimen is deformed and stable. Then, the axial pressure is loaded to the preset value at the rate of 0.1 kN/s, and the axial pressure of each stage is maintained for enough time until the axial strain is fixed, and then the next stage of axial pressure is loaded, and the last stage of axial pressure is loaded so that the sample is stopped after damage. Replace the rock sample, repeat the above steps for another experiment, and record the axial strain data during the experiment.

3.1. Creep Characteristics and Creep Strength. The creep curves of graded loading under different test conditions are shown in Figure 5. Due to space limitation, only 4 groups of creep curves are given in this paper, which represent the creep process when pH value, seepage pressure, and confining pressure cross change.

It can be seen from Figure 4 that the strain-time curve trend of all specimens in the whole creep process of red-bed soft rock is roughly similar. Under the same experimental conditions, with the increase of graded load, the steady creep rate of rock increases gradually, and the creep characteristics become more and more obvious. Especially when the last stage load is applied, the accelerated creep phenomenon is obvious. The duration of the creep failure stage is short, but the deformation is large.

When the stress and seepage pressure are the same, the more acidic the solution is, the more obvious the corrosion damage to red-bed soft rock is. The instantaneous deformation and creep deformation of the sample increase, the creep characteristics become more obvious, and the duration of the instability failure stage is shorter. When pH value and seepage pressure remain unchanged and confining pressure increases from 1.5 MPa to 3.5 MPa, creep strain decreases. When the fourth-stage load is applied, the increase of confining pressure prolongates the creep stabilization time. When pH value and confining pressure remain unchanged and seepage pressure increases, creep curve morphology changes little under the first four loads, but creep strain increases slightly. When the fifth-order load is applied, the duration of the accelerated creep phase is obviously shortened, the creep strength is obviously reduced, and the creep deformation is also increased.

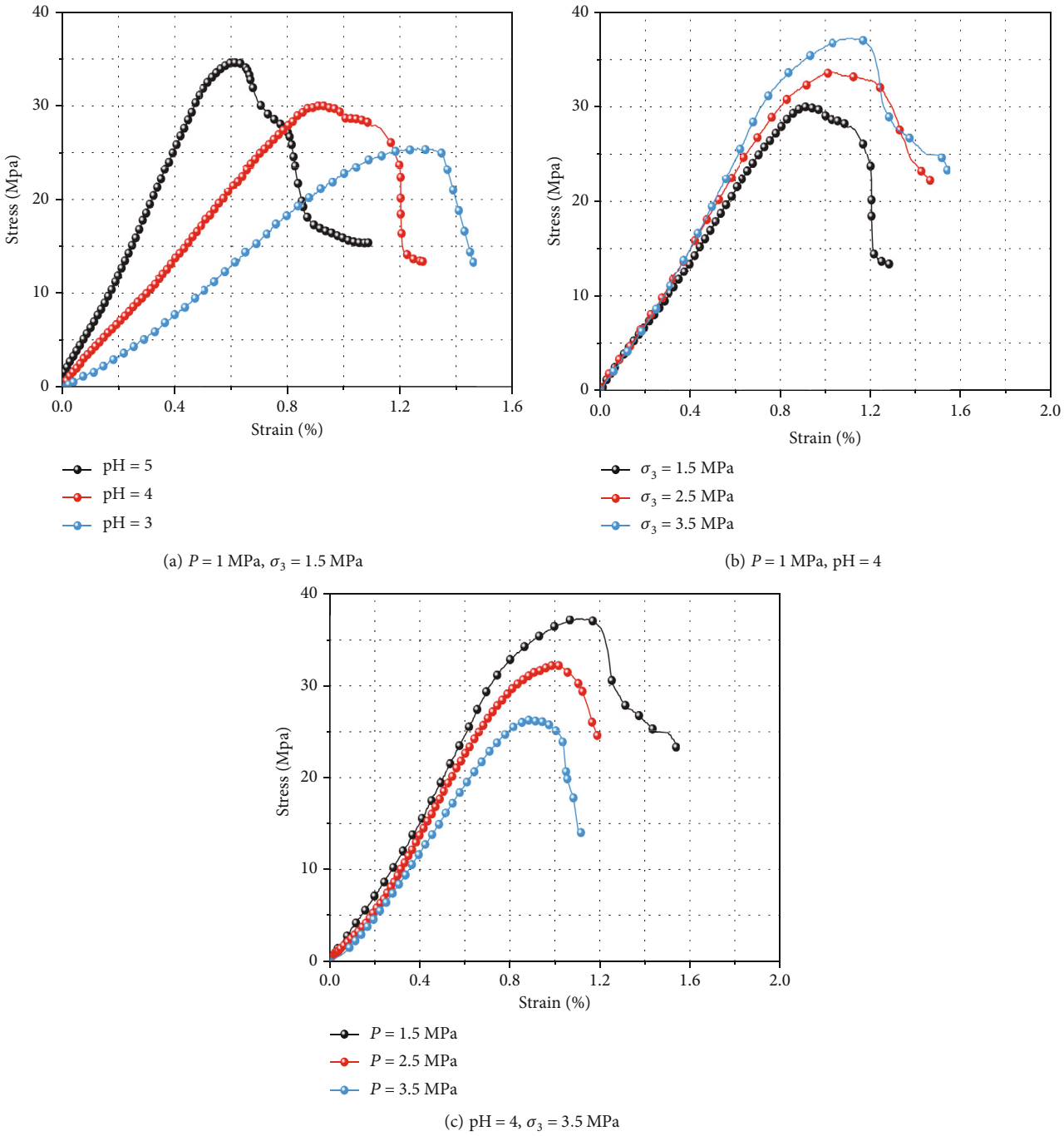

(a) P = 1 MPa, σ_3 = 1.5 MPa

(b) P = 1 MPa, pH = 4

(c) pH = 4, σ_3 = 3.5 MPa

Figure 4: Triaxial stress-strain curves under different experimental conditions.

3.2. The Strain and Strength of Creep

3.2.1. Creep Strain. The strain generated at each stress level is divided into two parts: instantaneous strain and creep strain. Then, the strain increment can be expressed as

$$\Delta\varepsilon_i = \Delta\varepsilon_{i1} + \Delta\varepsilon_{i2}, \quad (1)$$

where $\Delta\varepsilon_i$ is the total strain increment at each level, $\Delta\varepsilon_{i1}$ is the instantaneous strain increment at each level, and $\Delta\varepsilon_{i2}$ is the creep strain increment at each level.

The test results at the fourth stress level were taken as an example (Table 2) to compare the composition of strain increments at each stress level. The absolute values of instantaneous strain and creep strain are different, but their proportion in the total strain increment is about 50%. The more acidic the chemical solution is, the more serious the corrosion degree of the internal structure of the rock, the larger the total strain increment, and the instantaneous strain slightly predominates. With the increase of confining pressure, the total strain increment decreases slightly but has little effect on the proportion of instantaneous strain

Table 1: Test results of compressive mechanical properties of red-bed soft rock.

Group	pH	σ_3/MPa	P/MPa	(σ_1-σ_3)/MPa
A1	3	1.5	1.0	25.42
A2	4	1.5	1.0	30.01
A3	5	1.5	1.0	34.68
B1	4	2.5	1.0	33.98
B2	4	3.5	1.0	37.23
C1	4	3.5	2.0	32.19
C2	4	3.5	3.0	26.57

σ_3: confining pressure; P: seepage pressure; (σ_1 - σ_3): deviatoric stress.

and creep strain. With the increase of seepage pressure, the rock sample particles are more prone to dislocation slip, the total strain increment is larger, and the creep strain is slightly dominant.

3.2.2. Creep Strength. Under the creep condition under fractional loading, the creep strength of the sample is between the failure stress level and the previous stress level and is related to the action time of the failure stress level. The calculation relationship is as follows:

$$\sigma_T = \sigma_{n-1} + (\sigma_n - \sigma_{n-1})\frac{t}{T}, \tag{2}$$

where σ_T is the creep strength of the specimen, MPa; σ_n is the destructive stress level, MPa; t is the duration of the destructive stress level, h; and T is the creep time per stress level, h.

The calculation results of creep strength are shown in Table 3.

According to the calculation results of creep strength, increasing the acidity of the chemical solution is the most unfavorable to the bearing capacity of the sample; not only does the strength decrease obviously, but also the duration of the accelerated creep stage is the shortest. The second unfavorable factor is the seepage pressure, while the confining pressure is beneficial to the lifting capacity. The internal structure of the specimen underwent complex changes in the creep process under the coupled action of chemical-stress-seepage. Firstly, the acidic solution corrodes the pore structure and skeleton, enhances the seepage channel, and degrades the mechanical properties. Secondly, the seepage channel of red-bed soft rock is blocked by the compaction of low axial pressure and confining pressure, and the seepage pressure becomes the reaction of axial pressure and confining pressure, and the deterioration of seepage is inhibited. Then, higher axial pressure and creep damage caused the formation and expansion of cracks inside the sample, and the seepage channel was opened and strengthened again. Chemical corrosion, axial pressure loading, and fluid erosion formed a combined force to destroy the sample.

4. Evolution Characteristics of Creep Energy

4.1. Principle of Energy Dissipation in Creep under Fractional Loading. According to the first law of thermodynamics, assuming that there is no heat exchange between the test system and the outside, the total energy $U_\varkappa$ input by the testing machine to do work on the specimen is converted into elastic energy U_e and dissipative energy U_d. Among them, the elastic strain energy is stored in the specimen, and the dissipative energy is dissipated or released with the structural adjustment, damage, deformation, and deformation failure of the rock. Under the creep condition of graded loading, $U_\varkappa$ includes the work done by the testing machine on the specimen in the loading stage and the creep stage, which are, respectively, as follows U_l and U_c. Dissipative energy can be divided into load-phase dissipative energy U_{dl} and creep-phase dissipative energy U_{dc}. Therefore, the energy inside the sample at each stress level satisfies the following relationship:

$$\begin{aligned} U_\varkappa &= U_e + U_d = U_l + U_c, \\ U_d &= U_{dl} + U_{dc}. \end{aligned} \tag{3}$$

The destruction of the specimen is inevitably accompanied by energy dissipation, and the dissipated energy can be used as an important indicator of specimen damage. Through a series of cyclic loading and unloading tests, surface rock loading exists in the linear energy storage law [17, 18]. That is, the elastic energy U_{ie} input into the specimen during loading is linearly related to the total energy U_{iz}.

$$U_{ie} = kU_{iz} + b, \tag{4}$$

where the slope of the straight line k is the energy storage coefficient, representing the ability of the specimen to store elastic energy, the intercept b is generally negligible, and i is the different loading levels.

The simplified linear energy storage law can be expressed as the ratio of the elastic energy U_{ie} or dissipated energy U_{id} to the total input energy U_{iz}, which is a constant value. That is, $U_{ie}/U_{il} = k$ or $U_{id}/U_{il} = 1 - k$. The above results provide ideas for the calculation of energy under graded loading creep conditions.

Based on the principle of linear energy storage, combined with the graded loading creep stress/strain relationship in Figure 6, the whole process loading path of step loading creep is drawn, as shown in Figure 7, and then the total energy, elastic energy, and dissipative energy of the stepwise loading creep test are calculated.

Based on the principle of linear energy storage, the influence of the creep stage on elastic energy is ignored, and the loading stage is assumed to be the linear elastic stage; that is, the elastic modulus of each stage E_i is expressed as

$$E_i = \frac{\Delta\sigma_i}{\Delta\varepsilon_i} = \frac{(\sigma_i - \sigma_{i-1})}{(\varepsilon_{il} - \varepsilon_{i0})}, \tag{5}$$

where σ_i is the stress applied at each loading stage and ε_i is the strain applied at each loading stage.

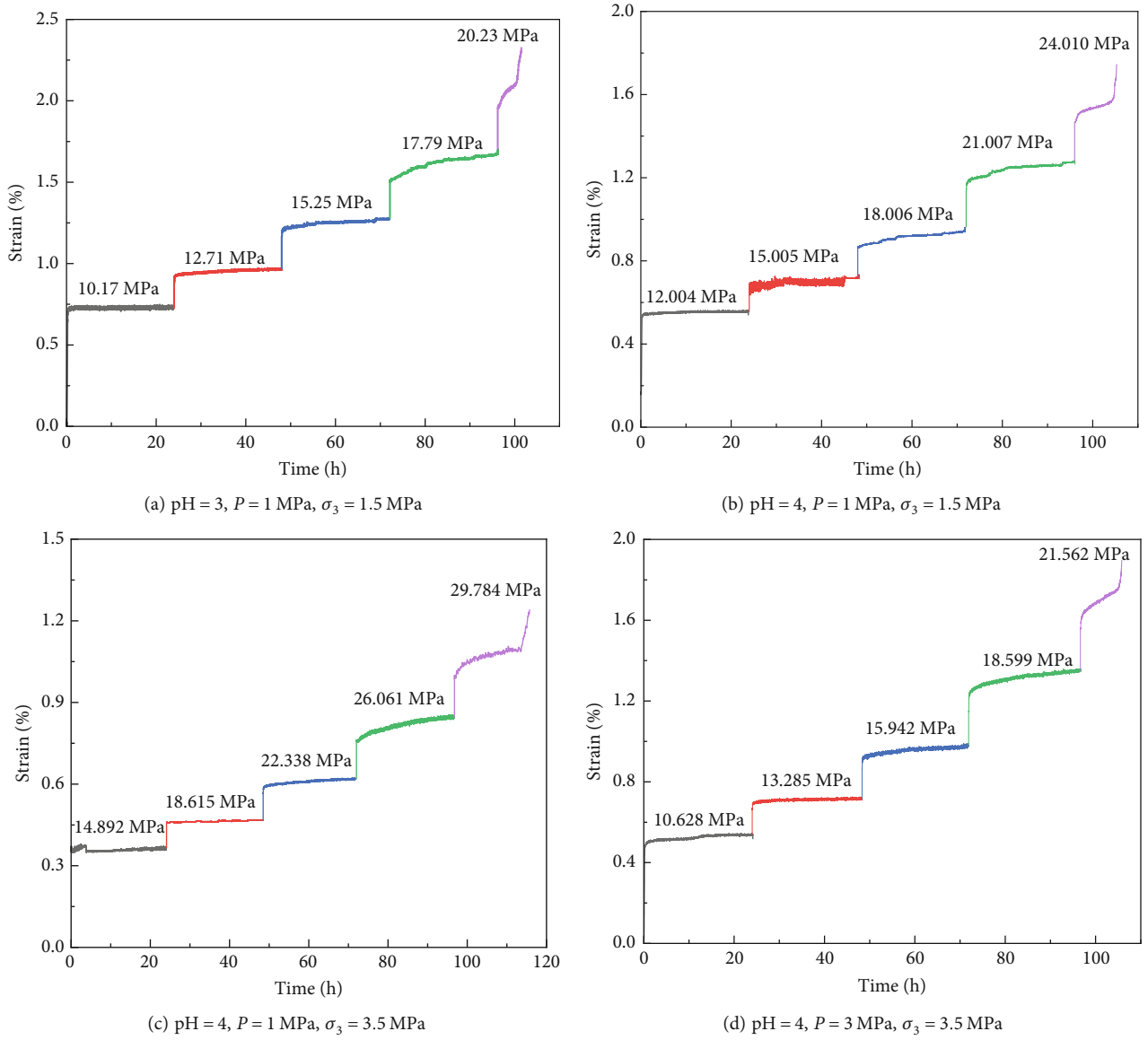

(a) pH = 3, P = 1 MPa, σ_3 = 1.5 MPa

(b) pH = 4, P = 1 MPa, σ_3 = 1.5 MPa

(c) pH = 4, P = 1 MPa, σ_3 = 3.5 MPa

(d) pH = 4, P = 3 MPa, σ_3 = 3.5 MPa

Figure 5: Graded loading creep test curve.

Table 2: Creep deformation under the fourth loading.

Group	$\Delta\varepsilon_i$	$\Delta\varepsilon_{i1}$		$\Delta\varepsilon_{i2}$	
		Value	Ratio/%	Value	Ratio/%
A1	0.427	0.225	52.69	0.203	47.54
A2	0.317	0.163	51.42	0.154	48.58
A3	0.241	0.119	49.38	0.122	50.62
B1	0.278	0.137	49.28	0.141	50.72
B2	0.227	0.123	54.19	0.105	46.26
C1	0.265	0.144	54.34	0.121	45.66
C2	0.369	0.170	46.07	0.199	53.93

Table 3: Calculation results of creep strength.

Group	Failure stress/MPa	Duration/h	Creep strength/MPa
A1	20.336	4.983	18.322
A2	24.01	9.316	22.173
A3	27.744	20.180	27.192
B1	27.184	13.975	25.765
B2	29.784	18.961	29.002
C1	25.752	13.98	24.408
C2	21.562	9.171	19.731

The relationship between the elastic/dissipative energy in the loading phase and the total energy input is

$$U_{ei} = kU_{zi} \quad \text{or} \quad U_{dli} = (1-k)U_{li}, \tag{6}$$

where k is the linear energy storage coefficient.

Then, the input total energy density U, elastic energy density U_e, and dissipated energy U_d are calculated as follows:

$$U = \int_{\varepsilon_{i0}}^{\varepsilon_{i1}} \sigma(\varepsilon) d\epsilon = \frac{E_i(\varepsilon_{il} - \varepsilon_{i0})^2}{2}, \tag{7}$$

$$U = U_e + U_d, \tag{8}$$

$$U_{ei} = \frac{1}{2E}\left(\sigma_1^2 - 4\upsilon\sigma_1\sigma_3\right), \tag{9}$$

$$U_d = U_{dci} + U_{dli}, \tag{10}$$

where ν is Poisson's ratio.

Furthermore, the dissipated energy density U_{dci} in the creep stage is calculated as follows:

$$U_{dci} \int_{\varepsilon_{i1}}^{\varepsilon_{i2}} \sigma_1 d\varepsilon, \tag{11}$$

where E_i is the modulus of elasticity of the specimen during the loading stage at different stress levels, U is the total energy density of the whole process, U_{ei} is the elastic energy density during the loading phase at different stress levels, and U_{dli} is the dissipated energy density during the loading phase at different stress levels.

4.2. Energy Storage Law in the Whole Process of Creep. According to formulas (5) and (7), the total energy density and elastic energy density of the specimen were calculated, respectively, and the energy storage curve drawn according to the calculation results is shown in Figure 8.

As shown in Figure 6, under the coupled condition of chemical-stress-seepage, the elastic energy density and total energy density of the sample meet a linear relationship; that is, the elastic energy density of each stress level increases linearly with the total energy density. The slope of the fitted line is the energy storage coefficient k. Specific data are shown in Table 4, which can quantitatively characterize the ability of the sample to convert the absorbed energy into elastic energy.

With the increase of pH value and confining pressure, the k value increases, but the k value decreases with the increase of seepage pressure. From the point of view of the mechanical energy storage of the rock body, the greater the rock strength, the better the elastic energy storage. It can be seen that solution acidity and seepage pressure weaken the rock strength while confining pressure enhances the peak rock strength, which is consistent with the change in elastic modulus.

4.3. Characteristics of Energy Dissipation in the Whole Creep Process. From a mechanical point of view, the deformation and failure process of rock is an irreversible process of energy dissipation. The existence of rock energy storage capacity as an energy source medium significantly affects the stability of deformation and generally affects the mechanical properties of the deformation process. During the loading phase, the specimen continuously converts the work done by the external forces into elastic energy stored inside the specimen. With the increase of applied load, when the elastic energy stored in the sample exceeds its energy storage limit, the elastic energy is released, resulting in plastic failure and instability of the sample.

Based on equations (8) and (9), the dissipated energy density of the specimen at the loading stage and the creep stage was calculated, respectively, and the change curves of elastic energy density, the dissipated energy density at the loading stage, and the creep stage with time were drawn, as shown in Figure 9.

The elastic energy density and dissipated energy density at the loading stage and the creep stage all increase nonlinearly with the loading time, but the dissipated energy density is less than the elastic energy density. The dissipated energy in the loading stage is mainly used for internal structural adjustment, fracture generation, and expansion. With the continuous accumulation of specimen damage, the dissipated energy increases gradually. The dissipated energy in the creep stage is mainly used to produce plastic strain, which is directly related to the creep strain. In the low-stress stage, the dissipative energy of creep is lower than that of loading, which indicates that the internal structural adjustment of rock is dominant in this stage, and the creep stage usually shows stable creep. Under the continuous action of higher stress, the energy dissipation rate keeps increasing, and the dissipative energy of creep gradually exceeds the dissipative energy of loading, which indicates that the plastic deformation of the specimen becomes dominant and the creep stage turns to unstable creep.

4.4. Characterization of Creep Damage. From the thermodynamic point of view, the internal structural adjustment of red-bed soft rock and the generation and expansion of fissures are accompanied by energy dissipation, and the evolution of specimen damage is an energy-dissipating and irreversible process, which is the internal cause of specimen deformation and destruction. Under graded loading conditions, the damage of the specimen accumulates gradually with the loading level and creep; the higher the damage

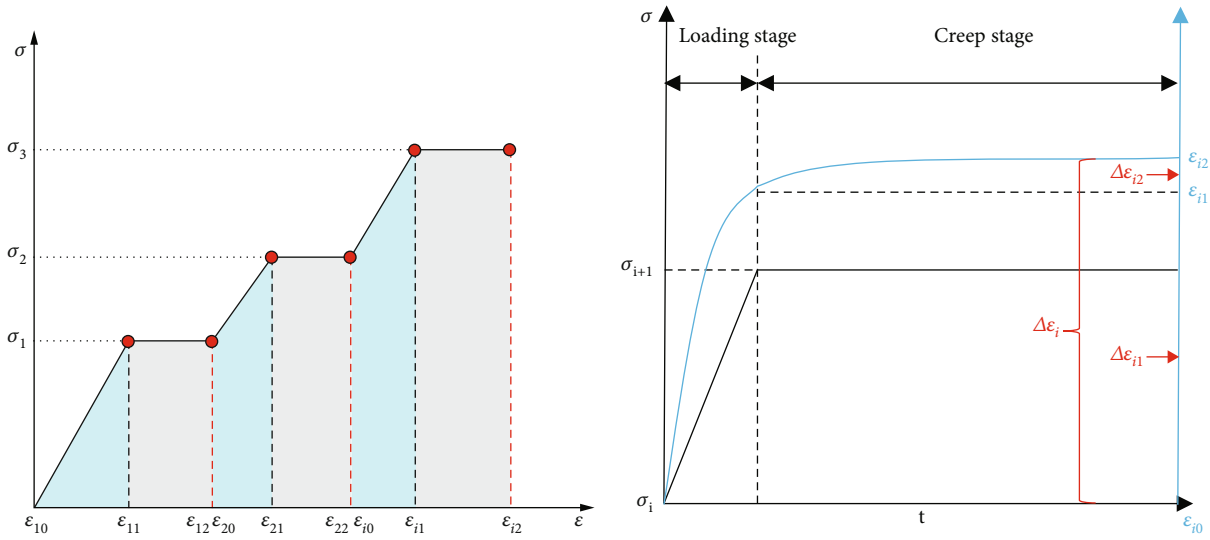

(a) Creep full course loading path (b) Single stress level stress/strain-time relationship

Figure 6: Graded loading creep stress/strain relationship.

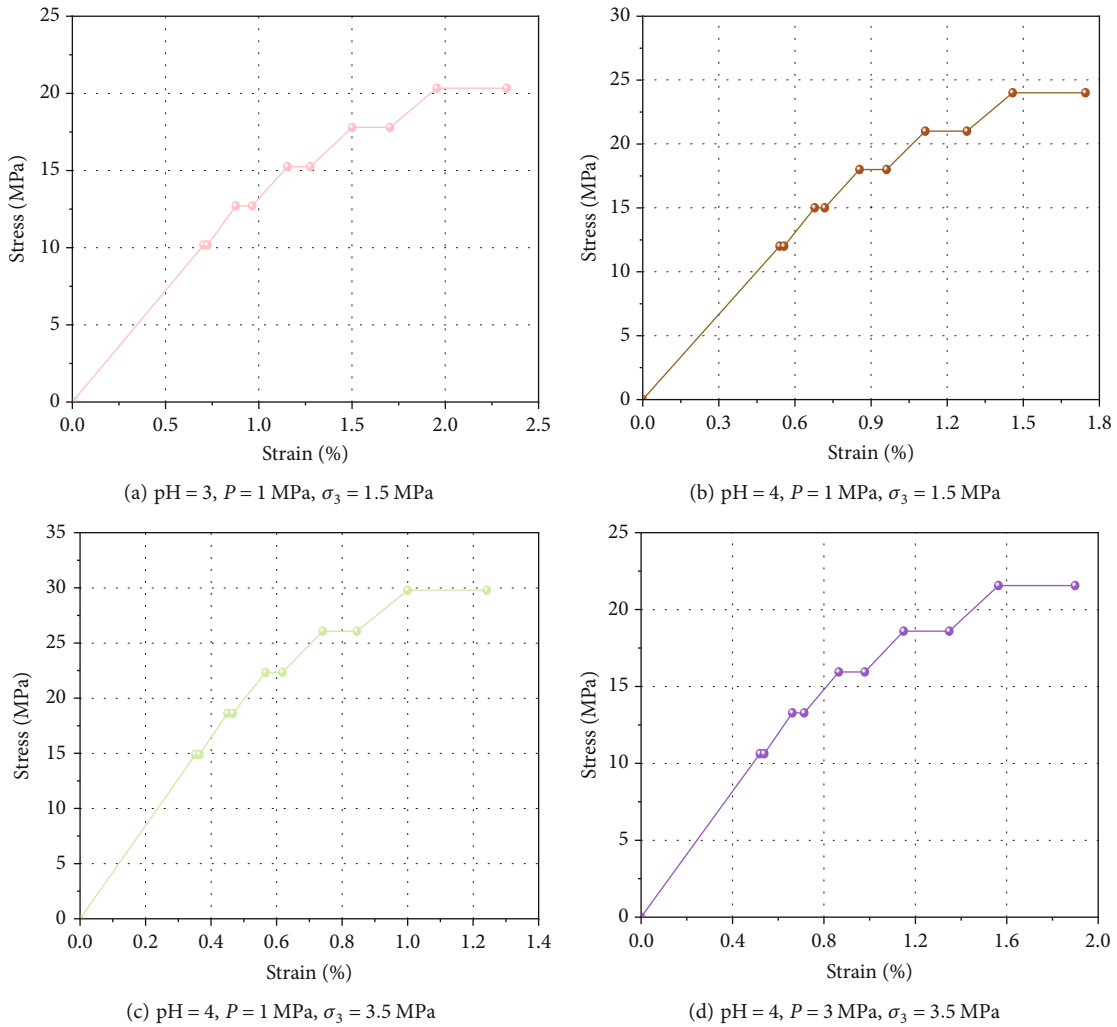

(a) pH = 3, P = 1 MPa, σ_3 = 1.5 MPa

(b) pH = 4, P = 1 MPa, σ_3 = 1.5 MPa

(c) pH = 4, P = 1 MPa, σ_3 = 3.5 MPa

(d) pH = 4, P = 3 MPa, σ_3 = 3.5 MPa

Figure 7: The whole process loading path of step loading creep.

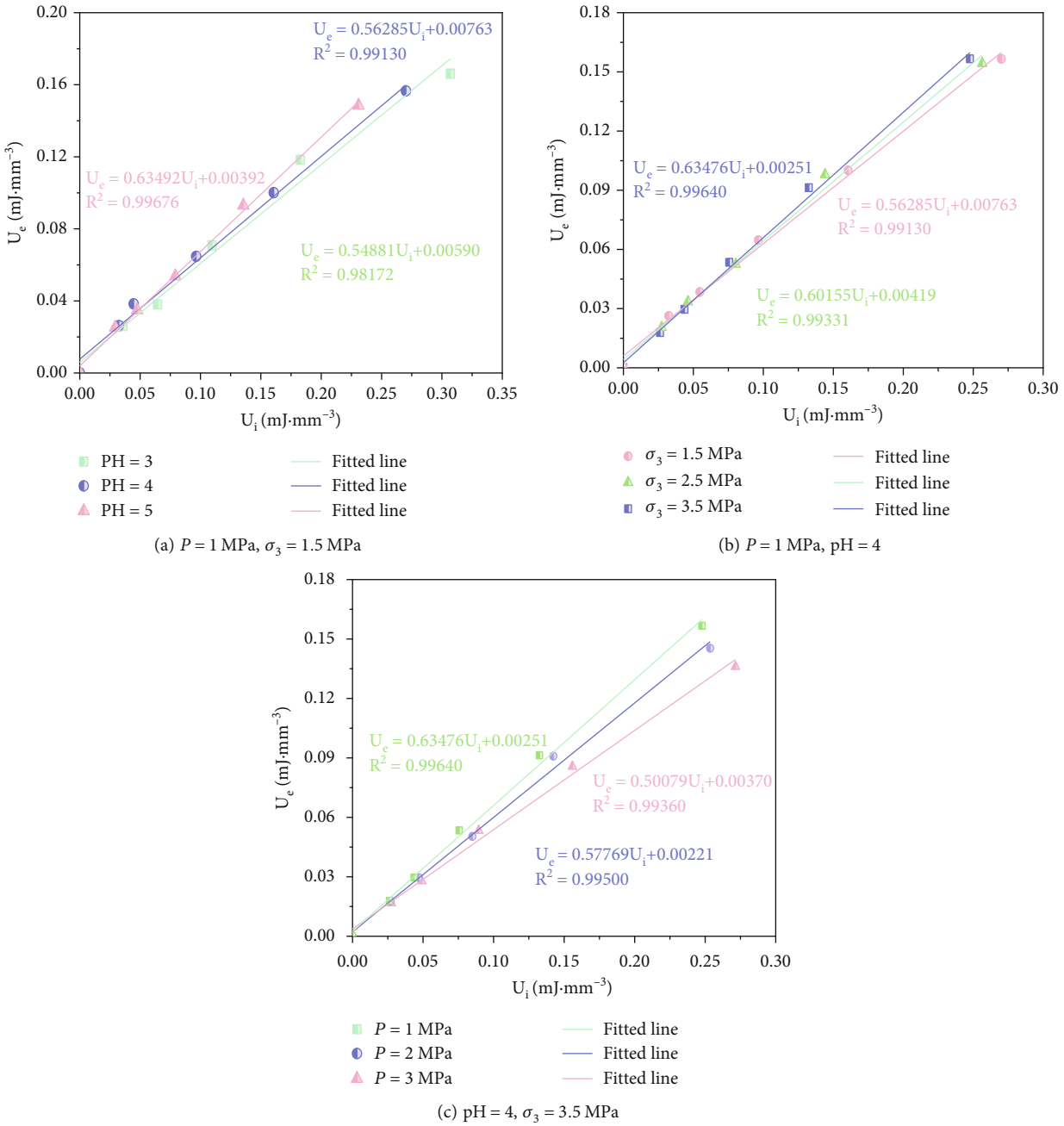

(a) P = 1 MPa, σ_3 = 1.5 MPa

(b) P = 1 MPa, pH = 4

(c) pH = 4, σ_3 = 3.5 MPa

Figure 8: Linear energy storage law for red-bed soft rock specimen.

Table 4: Energy storage coefficient under different experimental conditions.

Group	pH	σ_3/MPa	P/MPa	k
A1	3	1.5	1.0	0.54881
A2	4	1.5	1.0	0.56285
A3	5	1.5	1.0	0.63492
B1	4	2.5	1.0	0.60155
B2	4	3.5	1.0	0.63476
C1	4	3.5	2.0	0.57769
C2	4	3.5	3.0	0.50079

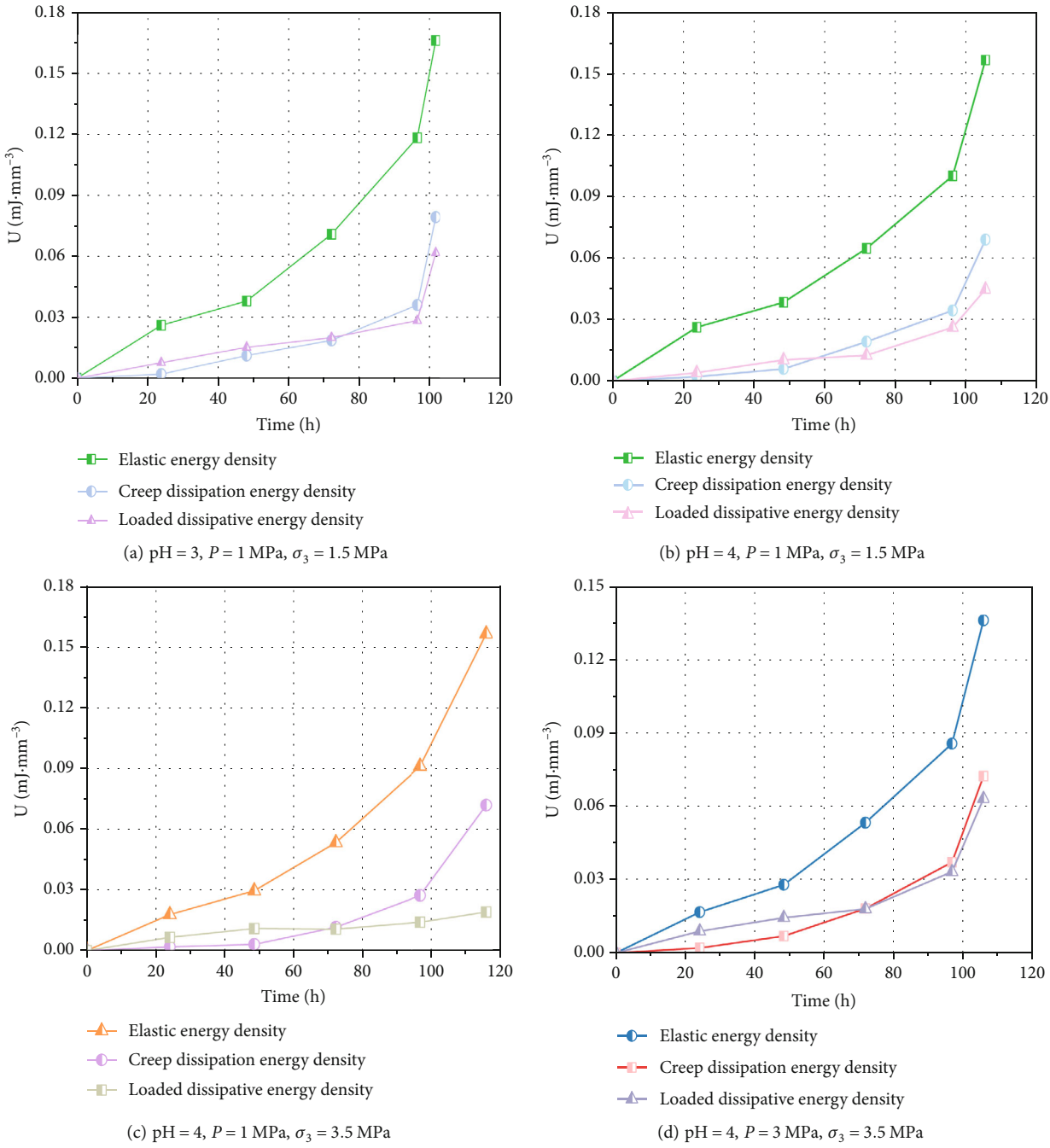

Figure 9: Evolution of energy density – time.

degree of the specimen, the more obvious the energy dissipation, the less elastic energy stored in the loading stage, and the lower the storage limit of the specimen. In order to quantitatively describe the damage evolution of the sample during the test, the ratio of dissipated energy U_d to the cumulative dissipated energy U_s at the moment of sample instability was defined as the energy damage variable D_u. In this paper, the initial damage of the sample is ignored, the pretest specimen damage variable is defined as 0, and the damage variable of the sample at the moment of creep instability is defined as 1. Under different stress levels, the damage variable of the sample can be characterized as

$$U_s = \sum_{i=1}^{n} (U_{dli} + U_{dci}),$$
$$D_{ui} = \frac{(U_{dli} + U_{dci})}{U_s}, \tag{12}$$

where U_s is the total dissipated energy density of the specimen at the moment of creep destabilization and D_{ui} is the damage variable at different stress levels.

The above formulas were used to calculate the damage variables in the whole process of creep under different stress

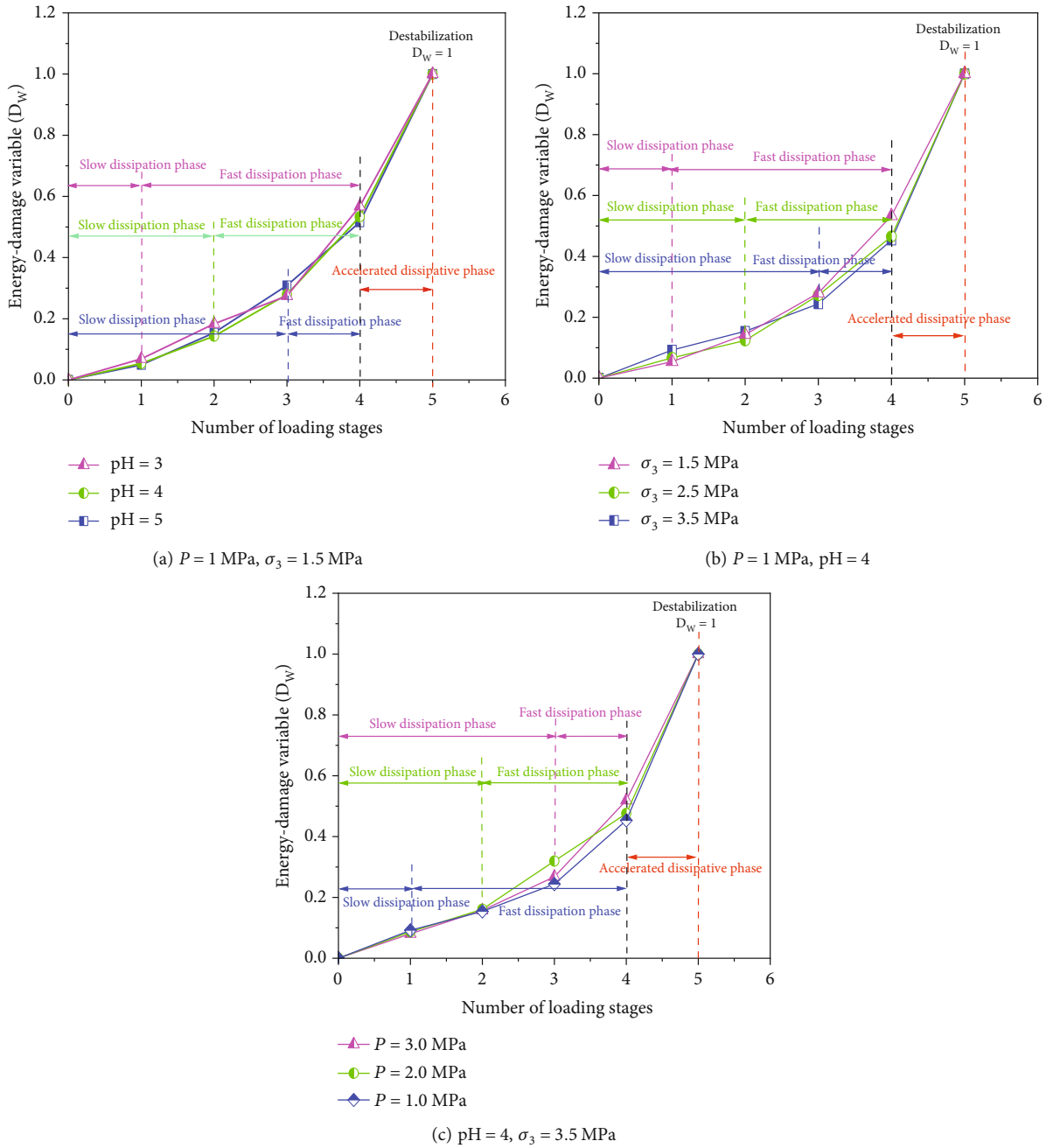

(a) P = 1 MPa, σ_3 = 1.5 MPa

(b) P = 1 MPa, pH = 4

(c) pH = 4, σ_3 = 3.5 MPa

Figure 10: Creep damage evolution curves at each loading stage.

levels, and the change curve of the sample damage variables was drawn, as shown in Figure 10.

With the increase of the level of graded loading stress, the creep of rock goes through three stages: deceleration creep, constant velocity creep, and accelerated creep, and the damage variables also increase slowly, accelerate, and rapidly. In the deceleration creep stage at a low-stress level, the damage variable slowly presents a linear increase, and the damage growth rate is similar. When the stress is applied to the creep stage of constant velocity, the damage growth rate is accelerated, and the difference in damage variables begins to appear. In the accelerated creep stage of the failure stress level, the slope of the curve increases further, and the damage occurs rapidly.

Due to the differences of the samples themselves, the damage variables were not strictly arranged in the order of pH value, confining pressure, and seepage pressure. In general, the stronger the acidity, the smaller the confining pressure, and the larger the seepage pressure, the greater the damage degree. In the phase of constant velocity creep, there is, on the one hand, the inherent damage caused by internal structure damage caused by loading, and on the other hand, the gradual damage caused by creep deformation, both of which work together to make obvious differences in damage variables.

4.5. The Harden-Damage Effect of Coupled Creep. Damage and hardening exist simultaneously in the creep process under fractional loading, and the two effects restrict the whole process of creep mutually. The hardening effect is mainly manifested in the increase of elastic modulus of red-bed soft rock in the loading stage, which is more conducive to energy storage and accumulation. The damage is reflected in the deterioration of the mechanical properties of the specimen. With the increase of the load level, the creep deformation continues to increase, and the creep rate gradually increases, resulting in a decrease in the viscosity coefficient, making it more prone to plastic failure, and a sudden increase in dissipated energy density. The different degrees of damage in specimens at different stress levels can well explain the phenomenon of increasing strain and accelerated creep. The deterioration of the specimen is more obvious at higher stress levels, and the damage effect is dominant.

During the graded loading creep test, both damage and hardening mechanisms coexist and constrain each other throughout the creep process. The damage of the specimen is accompanied by energy dissipation, and except for the damage level, the damage of the specimen shows a linear increase in relationship with the increase of the stress level, which fully indicates that the damage of the specimen has a transmission and accumulation nature. Therefore, when adopting the graded loading method to study the creep damage of red-layer soft rock, the cumulative effect of damage in the history of loading and creep stages should be considered.

The damage of the specimen is essentially a continuous energy-consuming process; the specimen creep damage is transmissive and cumulative. As can be seen from the figure, in addition to the accelerated creep stage, the damage degree of the specimen with the increase in the load level is approximately a linear growth relationship. In this paper, when the graded loading creep test is used to study the creep damage of red-layer soft rock, the cumulative effect of damage in the history of loading and creep stages should be considered comprehensively.

From Figure 9, it can be observed that in the middle of loading, when the stress level is at the middle-stress level, the elastic energy of the specimen accumulates a lot, which is due to the fact that at this time the elastic energy is increasing, leading to a significant enhancement of the hardening effect. However, the dissipated energy in the loading phase of this stage also increases gradually, so at this time, the damage effect and the hardening effect of the specimen are constrained by each other. When the specimen enters the late stage of loading, the stress level gradually grows to the level of destructive stress; at this time, the dissipated energy increases significantly, and the damage effect of the specimen dominates at this stage.

The influence of chemical-stress-seepage coupling on the hardening-damage effect is mainly reflected in the elastic modulus of the sample and the actual yield stress. The changes in pH value, confining pressure, and seepage pressure affect the rock structure to different degrees. The higher the damage degree, the more obvious the elastic modulus hardening effect at the initial loading stage, the higher the elastic energy storage efficiency of the sample, and the energy storage limit will also increase. At the same time, the damage also leads to the reduction of yield stress, and the accelerated creep stage is more easily induced under the same conditions, which accelerates the creep failure and energy dissipation process of the sample.

5. Conclusion

(1) The acidity of the chemical solution has the greatest effect on the triaxial strength and creep strength of the red-bedded soft rock in South China, causing irreversible damage. Creep damage increases with increasing acidity, decreasing confining pressure, and increasing seepage pressure, and the ability of absorbed mechanical energy to be converted into elastic energy decreases with a corresponding increase in the total strain increment. In addition, when acidity increases, the transient strain accounts for a larger proportion of the total strain. When the seepage pressure increases, creep strain accounts for a larger proportion of the total strain

(2) During the chemical-stress-percolation creep process, the damage growth shows "slow-accelerating-rapid," which is transmissive and cumulative with the increase in loading level. In the creep stage, the damage growth rate is accelerated, and the difference in damage variables appears

(3) In the step-loading creep process, there is a linear relationship between the elastic energy density and the total energy density, and the elastic energy density and the dissipated energy density in the loading stage and the creep stage all increase nonlinearly with the loading time. The energy dissipation law can explain the "hardening-damage" effect in the creep process of red bed chondrite samples

(4) In the low-stress stage, the loading energy is mainly used for the adjustment of the internal structure of the specimen, the deterioration of mechanical properties by seepage is suppressed, and the creep dissipation energy is lower than the loading dissipation energy. In the higher stress stage, the seepage channel increases with the crack extension, the energy dissipation rate increases, and the creep dissipation energy gradually exceeds the loading dissipation energy

Data Availability

The data used to support the findings of this study are available from the corresponding author upon request.

Conflicts of Interest

The authors declare that they have no conflicts of interest.

Acknowledgments

The study was supported by the National Natural Science Foundation of China (No. 42067041).

References

[1] X. S. Xie, H. S. Chen, X. H. Xiao, J. Wang, and J. W. Zhou, "Research on microstructural characteristics and softening mechanism of red bedded soft rock under water-rock coupling," *Journal of Engineering Geology*, vol. 27, no. 5, pp. 966–972, 2019.

[2] Z. Z. Cao, P. S. Wang, Z. H. Li, and F. Du, "Migration mechanism of grouting slurry and permeability reduction in mining fractured rock mass," *Scientific Reports*, vol. 14, no. 1, p. 3446, 2024.

[3] L. C. Wang, W. Zhang, Z. Z. Cao et al., "Effect of weakening characteristics of mechanical properties of granite under the action of liquid nitrogen," *Frontiers in Ecology and Evolution*, vol. 11, 2023.

[4] D. Qu, Y. Luo, X. P. Li, G. Wang, G. Zhang, and K. Xu, "Study on the stability of rock slope under the coupling of stress field, seepage field, temperature field and chemical field," *Arabian Journal for Science and Engineering*, vol. 45, no. 10, pp. 8315–8329, 2020.

[5] M. L. Zhou, J. L. Li, Z. S. Luo et al., "Impact of water–rock interaction on the pore structures of red-bed soft rock," *Scientific Reports*, vol. 11, no. 1, pp. 2045–2322, 2021.

[6] F. Gao, Q. Wang, H. W. Deng, J. Zhang, W. G. Tian, and B. Ke, "Coupled effects of chemical environments and freeze–thaw cycles on damage characteristics of red sandstone," *Bulletin of Engineering Geology and the Environment*, vol. 76, no. 4, pp. 1481–1490, 2017.

[7] Z. Liu, J. Liao, C. Xia, C. Y. Zhou, and L. H. Zhang, "Micro-meso-macroscale correlation mechanism of red-bed soft rocks failure within static water based on energy analysis," *Acta Geotechnica*, vol. 18, no. 12, pp. 6457–6474, 2023.

[8] N. Li, Y. M. Zhu, B. Su, and S. Gunter, "A chemical damage model of sandstone in acid solution," *International Journal of Rock Mechanics and Mining Sciences*, vol. 40, no. 2, pp. 243–249, 2003.

[9] Y. L. Chen, H. D. Tong, Q. J. Chen, X. Chen, and S. R. Wang, "Chemical corrosion-water-confining pressure coupling damage constitutive model of rock based on the SMP strength criterion," *Materials*, vol. 16, no. 18, p. 6234, 2023.

[10] C. Y. Zhou, Z. Y. Peng, W. Shang, and X. S. Tan, "On the mechanical variability of special soft rock as a focal point of water-rock interaction research in geotechnical engineering," *Geotechnics*, vol. 1, pp. 124–128, 2002.

[11] S. G. Zhang, Y. Xiao, Y. Song, W. B. Liu, and L. Yang, "Fluid-structure coupling creep characteristics of red-bed soft rock in South China," *Water*, vol. 14, no. 24, p. 4088, 2022.

[12] Z. G. Sun and H. T. Lu, "Experimental study on creep characteristics of red sandstone under water-rock chemical corrosion damage," *Metal Mining*, vol. 50, no. 4, pp. 83–89, 2021.

[13] H. F. Deng, M. L. Zhou, J. L. Li, X. S. Sun, and Y. L. Huang, "Creep degradation mechanism by water-rock interaction in the red-layer soft rock," *Arabian Journal of Geosciences*, vol. 9, no. 12, p. 601, 2016.

[14] H. P. Xie, L. Y. Li, R. D. Peng, and Y. Ju, "Energy analysis and criteria for structural failure of rocks," *Journal of Rock Mechanics and Geotechnical Engineering*, vol. 1, no. 1, pp. 11–20, 2009.

[15] Q. Xu, A. R. Tian, X. Y. Luo, X. Liao, and Q. Tang, "Chemical damage constitutive model establishment and the energy analysis of rocks under water–rock interaction," *Energies*, vol. 15, no. 24, p. 9386, 2022.

[16] T. Wen, H. M. Tang, J. W. Ma, and Y. R. Liu, "Energy analysis of the deformation and failure process of sandstone and damage constitutive model," *KSCE Journal of Civil Engineering*, vol. 23, no. 2, pp. 513–524, 2019.

[17] L. Gao, F. Gao, Y. Xing, and Z. Z. Zhang, "An energy preservation index for evaluating the rockburst potential based on energy evolution," *Energies*, vol. 13, no. 14, p. 3636, 2020.

[18] F. Q. Gong, P. L. Zhang, and L. Xu, "Damage constitutive model of brittle rock under uniaxial compression based on linear energy dissipation law," *International Journal of Rock Mechanics and Mining Sciences*, vol. 160, article 105273, 2022.

[19] F. Q. Gong, J. Y. Yan, S. Luo, and X. B. Li, "Investigation on the linear energy storage and dissipation laws of rock materials under uniaxial compression," *Rock Mechanics and Rock Engineering*, vol. 52, no. 11, pp. 4237–4255, 2019.

[20] F. Q. Gong, J. Y. Yan, X. B. Li, and S. Luo, "A peak-strength strain energy storage index for rock burst proneness of rock materials," *International Journal of Rock Mechanics and Mining Sciences*, vol. 117, pp. 76–89, 2019.

[21] L. C. Wang, X. Yi, Z. Z. Cao, H. L. Kong, J. Y. Han, and Z. Z. Zhang, "Experimental study on mode I fracture characteristics of granite after low temperature cooling with liquid nitrogen," *Water*, vol. 15, no. 19, p. 3442, 2023.

[22] Z. X. Liu, G. M. Zhao, X. R. Meng et al., "Analysis method of creep energy evolution of red sandstone based on linear energy storage law," *Journal of Central South University*, vol. 52, no. 8, pp. 2748–2760, 2021.

[23] J. Wang, J. T. Li, Z. M. Shi, and J. C. Chen, "Energy evolution and failure characteristics of red sandstone under discontinuous multilevel fatigue loading," *International Journal of Fatigue*, vol. 160, article 106830, 2022.

[24] C. Han, D. M. Pang, and D. J. Li, "Analysis of energy evolution during graded loading and unloading creep tests in sandstone," *Geotechnics*, vol. 41, no. 4, pp. 1179–1188, 2020.

[25] R. K. Huo, Y. L. Liang, S. G. Li, Z. Z. Miao, and T. Qiu, "The damage mechanism and deterioration characteristics of acid-corroded sandstone: an experimental study," *Arabian Journal of Geosciences*, vol. 15, no. 6, p. 537, 2022.

[26] Y. L. Zhao, T. Tan, C. Y. Zhang, Q. Liu, Y. J. Zhang, and L. H. Wu, "Mechanical properties and energy evolution and the applicability of strength criteria of sandstone under hydro-mechanical coupling," *Journal of China Coal Society*, vol. 48, no. 9, pp. 3323–3335, 2023.

[27] Y. L. Chen, Q. J. Chen, P. Xiao, X. Du, and S. R. Wang, "Chemical corrosion-confining pressure damage constitutive model and discrete element simulation of rock," *Chinese Journal of Solid Mechanics*, vol. 43, no. 6, pp. 703–715, 2022.

[28] W. G. Liang, M. Y. Cao, X. Q. Yang, C. D. Zhang, and S. G. Xu, "Experimental study on creep of glauberite salt rock under coupled compression and dissolution," *Chinese Journal of Rock Mechanics and Engineering*, vol. 35, no. 12, pp. 2461–2470, 2016.